Title

Entorhinal Tau Pathology, Episodic Memory Decline, and Neurodegeneration in Aging

Journal

Journal of Neuroscience, 38(3)

ISSN

0270-6474

Authors

Maass, Anne
Lockhart, Samuel N
Harrison, Theresa M
et al.

Publication Date

2018-01-17

DOI

10.1523/jneurosci.2028-17.2017

Peer reviewed

Neurobiology of Disease

Entorhinal Tau Pathology, Episodic Memory Decline, and Neurodegeneration in Aging

Anne Maass,[1,2] Samuel N. Lockhart,[1,3] Theresa M. Harrison,[1] Rachel K. Bell,[1] Taylor Mellinger,[1] Kaitlin Swinnerton,[1] Suzanne L. Baker,[4] Gil D. Rabinovici,[1,5] and William J. Jagust[1,4]

[1]Helen Wills Neuroscience Institute, University of California Berkeley, Berkeley, California 94720, [2]German Center for Neurodegenerative Diseases, Magdeburg 39120, Germany, [3]Department of Internal Medicine, Division of Gerontology and Geriatric Medicine, Wake Forest School of Medicine, Winston-Salem, North Carolina 27157, [4]Molecular Biophysics and Integrated Bioimaging, Lawrence Berkeley National Laboratory, Berkeley, California 94720, and [5]Memory and Aging Center, University of California San Francisco, San Francisco, California 94158

The medial temporal lobe (MTL) is an early site of tau accumulation and MTL dysfunction may underlie episodic-memory decline in aging and dementia. Postmortem data indicate that tau pathology in the transentorhinal cortex is common by age 60, whereas spread to neocortical regions and worsening of cognition is associated with β-amyloid (Aβ). We used [^{18}F]AV-1451 and [^{11}C]PiB positron emission tomography, structural MRI, and neuropsychological assessment to investigate how *in vivo* tau accumulation in temporal lobe regions, Aβ, and MTL atrophy contribute to episodic memory in cognitively normal older adults ($n = 83$; age, 77 ± 6 years; 58% female). Stepwise regressions identified tau in MTL regions known to be affected in old age as the best predictor of episodic-memory performance independent of Aβ status. There was no interactive effect of MTL tau with Aβ on memory. Higher MTL tau was related to higher age in the subjects without evidence of Aβ. Among temporal lobe subregions, episodic memory was most strongly related to tau-tracer uptake in the parahippocampal gyrus, particularly the posterior entorhinal cortex, which in our parcellation includes the transentorhinal cortex. In subjects with longitudinal MRI and cognitive data ($n = 57$), entorhinal atrophy mirrored patterns of tau pathology and their relationship with memory decline. Our data are consistent with neuropathological studies and further suggest that entorhinal tau pathology underlies memory decline in old age even without Aβ.

Key words: β-amyloid; aging; episodic memory; positron emission tomography; tau; transentorhinal cortex

Significance Statement

Tau tangles and β-amyloid (Aβ) plaques are key lesions in Alzheimer's disease (AD) but both pathologies also occur in cognitively normal older people. Neuropathological data indicate that tau tangles in the medial temporal lobe (MTL) underlie episodic-memory impairments in AD dementia. However, it remains unclear whether MTL tau pathology also accounts for memory impairments often seen in elderly people and how Aβ affects this relationship. Using tau-specific and Aβ-specific positron emission tomography tracers, we show that *in vivo* MTL tau pathology is associated with episodic-memory performance and MTL atrophy in cognitively normal adults, independent of Aβ. Our data point to MTL tau pathology, particularly in the entorhinal cortex, as a substrate of age-related episodic-memory loss.

Introduction

The ability to encode novel events into long-term memory declines in old age and this impairment is related to dysfunction of the medial temporal lobe (MTL) memory system (for review, see Hedden and Gabrieli, 2004; Small et al., 2011). Intriguingly, postmortem data indicate that tau neurofibrillary tangles (NFTs) emerge early in the transentorhinal cortex (Braak and Braak, 1985), the transition area between the entorhinal cortex (EC) and the perirhinal cortex. These early "transentorhinal stages" (Braak

Received July 7, 2017; revised Sept. 14, 2017; accepted Oct. 7, 2017.

Author contributions: G.D.R. and W.J.J. designed research; A.M., R.K.B., T.M., K.S., S.L.B., G.D.R., and W.J.J. performed research; A.M., S.N.L., T.M.H., R.K.B., and S.L.B. analyzed data; A.M., S.N.L., T.M.H., S.L.B., G.D.R., and W.J.J. wrote the paper.

This work was supported by the Helmholtz Postdoc Program (PD-306; to A.M.), Tau Consortium (to W.J.J. and G.D.R.), and National Institute on Aging Grants R01-AG045611 (to G.D.R.), R01AG034570 (to W.J.J.), P50-AG023501 (G.D.R.), and P01-AG1972403 (to W.J.J.). Avid Radiopharmaceuticals enabled use of the [^{18}F] AV-1451 tracer, but did not provide direct funding and were not involved in data analysis or interpretation.

G.D.R. receives research funding from Avid Radiopharmaceuticals, GE Healthcare, and Piramal. He has received consulting fees or speaking honoraria from Eisai, Genentech, Lundbeck, Putnam, Merck, and Roche. W.J.J. has served as a consultant to the Banner Alzheimer Institute, Genentech, Novartis, Bioclinica, and Merck.

Correspondence should be addressed to Anne Maass, Jagust Laboratory, Helen Wills Neuroscience Institute, 132 Barker Hall, MC #3190, University of California, Berkeley, Berkeley CA 94720-3190. E-mail: anne.maass@dzne.de.

DOI:10.1523/JNEUROSCI.2028-17.2017

 0270-6474/18/380530-14$15.00/0

stages I/II) of tau deposition are commonly observed in individuals ≥60 years old, while the spread of tau to limbic and neocortical areas is usually accompanied by the presence of β-amyloid (Aβ) plaques (Braak and Braak, 1997). While both tau tangles and Aβ plaques are major pathological markers of Alzheimer's disease (AD), Aβ deposition is only weakly related to cognition (Hedden et al., 2013). Neuropathological data in AD patients suggest that NFTs mediate the association of Aβ deposition and cognitive decline (Giannakopoulos et al., 2003; Bennett et al., 2004). In a sample of normal adults and patients with mild cognitive impairment (MCI) or AD, NFT density in the parahippocampal gyrus (PhG) was linearly related to episodic memory performance (Mitchell et al., 2002). Tau pathology restricted to MTL and limbic regions without Aβ pathology is also described as primary age-related tauopathy (PART; Crary et al., 2014). Neuropathological data showed that higher Braak stage is related to higher age, worse cognition, and hippocampal (HC) head atrophy in cases with PART (Josephs et al., 2017). However, there is still debate about whether PART represents a non-AD entity that can be separated from early AD (Duyckaerts et al., 2015).

The advent of tau-specific positron emission tomography (PET) tracers enables the study of regional associations between tau pathology and cognition *in vivo*. Consistent with neuropathological data, tau PET studies have reported that most cognitively normal elderly adults demonstrate elevated tracer binding confined to the MTL, whereas neocortical binding requires the presence of aggregated Aβ (e.g. Schöll et al., 2016; Sepulcre et al., 2016; Lockhart et al., 2017). In samples that included patients, tau PET signal was related to cognitive impairment (Brier et al., 2016; Cho et al., 2016a; Johnson et al., 2016; Ossenkoppele et al., 2016; Maass et al., 2017), in contrast to weaker associations seen with Aβ. Moreover, our laboratory has shown that increased tracer retention in the MTL relates to worse episodic-memory performance in a small sample of 33 cognitively healthy older adults (OAs; Schöll et al., 2016). It remains unclear whether Aβ and tau have interactive effects on episodic memory, and whether *in vivo* MTL tau pathology predicts episodic-memory performance even in subjects without evidence of Aβ pathology. Furthermore, the regional specificity of associations between episodic memory and *in vivo* tau pathology within the temporal lobe has not been examined yet.

In the current study of 83 cognitively normal OAs (age range, 60–93 years), we investigated the contributions of age, Aβ burden, regional tau burden, and MTL atrophy to episodic-memory performance as well as interactive effects of Aβ and tau on memory. Global cortical Aβ burden was measured with [^{11}C] Pittsburgh compound B (PiB) and regional tau load was assessed by [^{18}F] AV-1451 PET scans. Cross-sectional measures of MTL atrophy were assessed by entorhinal thickness and HC volume. Episodic-memory composite scores were calculated from recall performance in verbal and visual memory tasks. We aimed to determine which biomarker best predicted episodic-memory performance in clinically normal elderly and to examine the specificity of associations between biomarkers and episodic memory across modalities (verbal vs visual) and with other cognitive domains (working memory and executive function). We further investigated the regional specificity of the association between tau and episodic memory by parcellating the temporal lobe along the longitudinal and medial–lateral axes. In a subgroup of 57 subjects with longitudinal MRI and cognitive data, we finally assessed associations between tau measures, entorhinal-thickness change, and episodic-memory decline.

Materials and Methods

Participants

Our sample comprised 83 cognitively normal OAs from the Berkeley Aging Cohort Study (BACS), a longitudinal study of normal aging. Aspects of memory function were recently reported in a subset of 33 subjects (Schöll et al., 2016). Subjects underwent structural MRI, [^{18}F]AV-1451 and [^{11}C]PiB PET imaging, neuropsychological assessment, and standard laboratory blood tests including *APOE* genotyping (data missing for eight subjects). The Institutional Review Boards of the University of California, Berkeley and the Lawrence Berkeley National Laboratory approved the study and informed consent was obtained from all participants.

Eligibility requirements for inclusion into BACS comprise the following: no MRI or PET contraindications, living independently in the community, Mini-Mental State Examination score (Folstein et al., 1975) ≥25, within 1.5 SD of normative values on the California Verbal Learning Test (CVLT; Delis et al., 2000) and delayed recall from the visual reproduction (VR) test (Wechsler, 1997), absence of neurological or psychiatric illness, and lack of major medical illnesses and medications that affect cognition. Subjects who performed below the CVLT or VR cutoff in one follow-up session remained in the study as we were interested in biomarkers underlying age-related memory decline.

Data acquisition and preprocessing

Cognitive data. Cross-sectional neuropsychological data closest to the AV-1451 tau scan were used to calculate composite *Z* scores for episodic-memory, working-memory, and executive-function domains. Cognitive data were collected within 117 ± 87 d of the tau PET scan. For >85% of the subjects, the time lag was <6 months. For only one subject, time delay was >1 year (1.3 years). *Z* scores were calculated as the average of the Z-transformed individual test scores using mean and SD from the first cognitive session data of a larger sample of 164 BACS OA participants (age: 74 ± 6 years; education: 17 ± 2 years; 60% female) that also included the 83 OAs studied here.

The memory composite score comprised short-delay and long-delay (after 20 min) free recall of the CVLT and VR tests. The working-memory score included the WMS-III Digit Span test forward and backwards total score. The executive function composite score comprised the Digit-Symbol test (Smith, 1982), number correct in 60 s in the Stroop Interference Test (Stroop, 1938) and "Trail B minus A" score from the Trail Making Test (Reitan, 1985; score inverted after *Z*-transformation).

Fifty-seven of 83 OAs had longitudinal MRI as well as cognitive data (≥2 scans/testing sessions). These subjects had between 2 and 10 cognitive testing sessions (mean, 5.6 ± 2.2) over a period of 5.6 ± 2.5 years with an average delay of 1.3 ± 0.3 years between sessions. For these subjects with both available longitudinal MRI and cognitive data, we also assessed measures of episodic-memory change (using linear mixed-effects models to derive slopes).

MRI data. For all subjects 1 × 1 × 1-mm-resolution T1-weighted magnetization prepared rapid gradient echo (MPRAGE) images were acquired at 1.5 T at Lawrence Berkeley National Laboratory (Schöll et al., 2016). These images were used for definition of brain regions of interest (ROIs) and for both cross-sectional and longitudinal measurement of MTL atrophy.

All MPRAGE scans were processed with the FreeSurfer (v5.3.0; http://surfer.nmr.mgh.harvard.edu/) cross-sectional pipeline to derive ROIs in each subject's native space using the Desikan–Killiany atlas. ROIs were used for calculation of region-specific tau PET measures after partial volume correction (PVC; Baker et al., 2017a) and for PiB PET distribution volume ratio (DVR) summary measures. Within our PET preprocessing pipeline, the first T1 image of each subject is coregistered to the SPM "avg152T1.nii" (image derived from icbm_avg_152_t1_tal_lin.mnc) to align the head, while all subsequently acquired T1 images are coregistered to that first MRI of a subject. These coregistration parameters are also applied to the FreeSurfer-derived aparc+aseg.nii (which is used to derive regional tau PET measures). PET scans are coregistered to the MRI closest in time.

MRI images were also segmented into brain tissue types using SPM12 (Statistical Parametric Mapping; Wellcome Department of Cognitive

Neurology, London, England). Tissue segments for noncerebral tissues (CSF, soft tissue, bone) were subsequently used for PVC. Segmentations for gray matter, white matter, and CSF were summed to derive intracranial volume (ICV).

FreeSurfer output from the closest 1.5 T MRI scan was used to derive bilateral mean HC volume and entorhinal thickness as cross-sectional measures of MTL atrophy. MRI scans were acquired within 65 ± 128 d of the tau PET scan. HC volumes were corrected for ICV (to account for differences in head size) via the following linear equation: $Vol_{adj} = Vol_{raw(i)} - b(ICV_{(i)} - Mean\ ICV)$, where Vol_{adj} is the adjusted HC volume, $Vol_{raw(i)}$ is the original volume for an individual, b is the slope of HC volume regressed on ICV, and Mean ICV is the sample mean of ICV (Raz et al., 2015).

Fifty-seven of 83 OAs had longitudinal 1.5 T MRI data, with 2–5 scans (mean, 2.8 ± 0.9) over a period of 4.5 ± 2.6 years and an average delay of 2.3 ± 1.4 years between two MRI scans. To extract reliable longitudinal volume and thickness estimates, these T1 images were processed with the longitudinal FreeSurfer stream (Reuter et al., 2012). Specifically, unbiased within-subject template space and image (Reuter and Fischl, 2011) are created using robust, inverse consistent registration (Reuter et al., 2010).

PET data. A detailed description of AV-1451 tau PET and PiB Aβ PET acquisition for BACS/UCSF (University of California San Francisco) has been published previously (Ossenkoppele et al., 2016; Schöll et al., 2016). AV-1451 scans were collected within 49 ± 91 d of PiB. PiB and AV-1451 PET images were reconstructed using an ordered subset expectation maximization algorithm with weighted attenuation and smoothed with a 4 mm Gaussian kernel with scatter correction (calculated image resolution, 6.5 × 6.5 × 7.25 mm^3 using Hoffman phantom).

AV-1451 standardized uptake value ratio (SUVR) images were coregistered and resliced to the structural MRI closest in time, as mentioned previously. We created AV-1451 SUVR images based on mean uptake over 80–100 min postinjection (Shcherbinin et al., 2016; Baker et al., 2017b; Wooten et al., 2017) normalized by mean inferior cerebellar gray matter uptake. We excluded the superior portion of the cerebellar gray from our reference region as it showed frequent tracer binding (Baker et al., 2017a). We created the inferior cerebellar gray ROI from the reverse-normalized cerebellar SUIT (A Spatially Unbiased Atlas Template of the Cerebellum and Brainstem) template as described in detail by Baker et al. (2017a).

To derive Braak-ROI mean values consistent with our previously published preprocessing stream and Braak-based staging approach (Maass et al., 2017), SUVR images were smoothed with a 4.7 × 4.7 × 2.8 mm^3 FWHM kernel to achieve a resolution of 8 × 8 × 8 mm^3 (i.e., resolution of Alzheimer's Disease Neuroimaging Initiative data on which we validated our Braak thresholds). These smoothed SUVR images were partial volume (PV) corrected using the Geometric Transfer Matrix approach (Rousset et al., 1998) with FreeSurfer-derived ROIs as described by Baker et al. (2017a). Goals of the PVC were to correct for choroid plexus and basal ganglia signal bleeding into neighboring regions (such as the HC), to account for PV effects due to atrophy, and to correct for spillover from extracortical hotspots. PV-corrected ROI SUVR values were renormalized by PV-corrected inferior cerebellar gray. For analyses on temporal lobe subregional patterns of tau-tracer uptake, we used the unsmoothed SUVR images (as we wanted to keep highest possible resolution), which were also PV-corrected after parcellation of the temporal lobe.

Individual PiB frames were realigned, coregistered, and resliced to the closest structural MRI. DVRs for PiB images were generated with Logan graphical analysis on PiB frames corresponding to 35–90 min postinjection using a cerebellar gray matter reference region (Logan et al., 1996; Price et al., 2005). The global cortical PiB DVR was calculated as a weighted mean across FreeSurfer-derived frontal, temporal, parietal, and posterior cingulate cortical regions. Participants were classified as PiB-positive if their global PiB DVR was >1.065, a cutoff adapted from previous thresholds developed in our laboratory (Mormino et al., 2012; Villeneuve et al., 2015). We only included OAs with full dynamic PiB data.

AV-1451 uptake in Braak composite regions. We (Schöll et al., 2016; Maass et al., 2017) along with other laboratories (Cho et al., 2016b; Schwarz et al., 2016; Hoenig et al., 2017) have proposed approaches to summarizing tracer uptake in ROIs that parallel the Braak staging approach. Specifically, we calculated weighted bilateral mean SUVR values after PVC in native space from three composite ROIs that approximate anatomical definitions of Braak stages I/II, III/IV, and V/VI. FreeSurfer indices for the different Braak ROIs can be found in Baker et al. (2017a). We recently developed AV-1451 SUVR thresholds for each Braak ROI, based on data of AD patients and controls, to assign subjects to one of four stages (Schöll et al., 2016; Maass et al., 2017). The number of subjects classified to each stage is summarized in Table 1.

Table 1. Demographics (mean ± SD)

	All OAs	PiB^- OAs	PiB^+ OAs
n	83	47	36
Age (years)	77 ± 6	77 ± 8	77 ± 4
Gender (% female)	58	57	58
Education (years)*	17 ± 2	17 ± 2	16 ± 2
APOE (% of e4 carriers)*	32[a]	14[b]	64[c]
PiB DVR*	1.15 ± 0.23	1.01 ± 0.03	1.33 ± 0.25
Days between PiB and AV-1451	49 ± 91	54 ± 105	42 ± 70
HC volume (cm^3)	3.5 ± 0.5	3.6 ± 0.5	3.5 ± 0.5
Entorhinal thickness (cm^2)	3.3 ± 0.4	3.4 ± 0.4	3.3 ± 0.4
Days between MRI and AV-1451	65 ± 128	60 ± 98	71 ± 161
Mini-Mental State Examination	29 ± 1	29 ± 1	28.5 ± 1
CVLT early recall*	10 ± 4	10 ± 4	9 ± 3
CVLT late recall	10 ± 4	11 ± 4	10 ± 4
VR early recall	75 ± 15	76 ± 15	73 ± 16
VR late recall	55 ± 20	57 ± 21	52 ± 19
Episodic memory	−0.05 ± 0.93	0.08 ± 0.96	−0.23 ± 0.86
Executive function	0.08 ± 0.67	0.10 ± 1.00	0.05 ± 0.97
Working memory	−0.13 ± 1.04	−0.05 ± 1.10	−0.23 ± 1.10
Days between cognition and AV-1451	117 ± 87	114 ± 94	121 ± 78
AV-1451 Braak-based stage (*n* in $stage_0$ / $stage_{I/II}$ / $stage_{III/IV}$ / $stage_{V/VI}$)	18/51/14/0	13/31/3/0	5/20/11/0

PiB^- versus PiB^+ groups were compared using *t* test for continuous variables and χ^2 test for gender and *APOE* status (*$p < 0.05$). Subjects were also assigned to one of four stages by means of AV-1451 uptake in Braak-based composite regions (see Materials and Methods).

[a]Not available for eight subjects.

[b]Not available for five subjects.

[c]Not available for three subjects.

Parcellation of the temporal lobe. To examine associations between temporal lobe regional tau patterns and memory, we used the FreeSurfer-derived ROIs of the HC, the EC, the parahippocampal cortex (PHC), the fusiform gyrus (FuG), the inferior temporal gyrus (ITG), and the middle temporal gyrus (MTG; Desikan et al., 2006) and subdivided those along the longitudinal axis of the temporal lobe. This is shown schematically in Figure 1*A* and for the group T1 image in MNI space in Figure 1*B*. We used the most anterior, the middle, and the most posterior HC slice (Fig. 1, cut points 1–3) as landmarks to coronally slice each gyrus (PhG, FuG, ITG, and MTG) into four segments (ant, med, post, postHC). Slicing was performed for each hemisphere separately. These anatomical landmarks were chosen as they can be automatically determined (in Matlab) by use of the HC FreeSurfer segmentation.

The FreeSurfer-defined EC covers the anterior portion of the PhG, including the medial bank of the collateral sulcus, and thus also likely includes the transentorhinal region (Braak and Braak, 1985, 1991; Taylor and Probst, 2008), corresponding to Brodmann's area (BA) 35 or to the medial perirhinal cortex (Kivisaari et al., 2013). A protocol for segmentation of the transentorhinal cortex at 7 T has been published recently (Berron et al., 2017). Rostral and caudal boundaries of the FreeSurfer-defined EC are the rostral end of the collateral sulcus and amygdala, respectively. The FreeSurfer-labeled "parahippocampal cortex" (which is called "parahippocampal gyrus" in the original paper by Desikan et al., 2006) is the posterior portion of the PhG, which borders the EC. We merged FreeSurfer EC and PHC ROIs before parcellation to derive a continuous PhG ROI.

Moving from anterior to posterior, the "ant" segment of each gyrus starts at its FreeSurfer-defined anterior boundary and ends on the first (most anterior) slice of the HC. The "med" segment ends on the middle

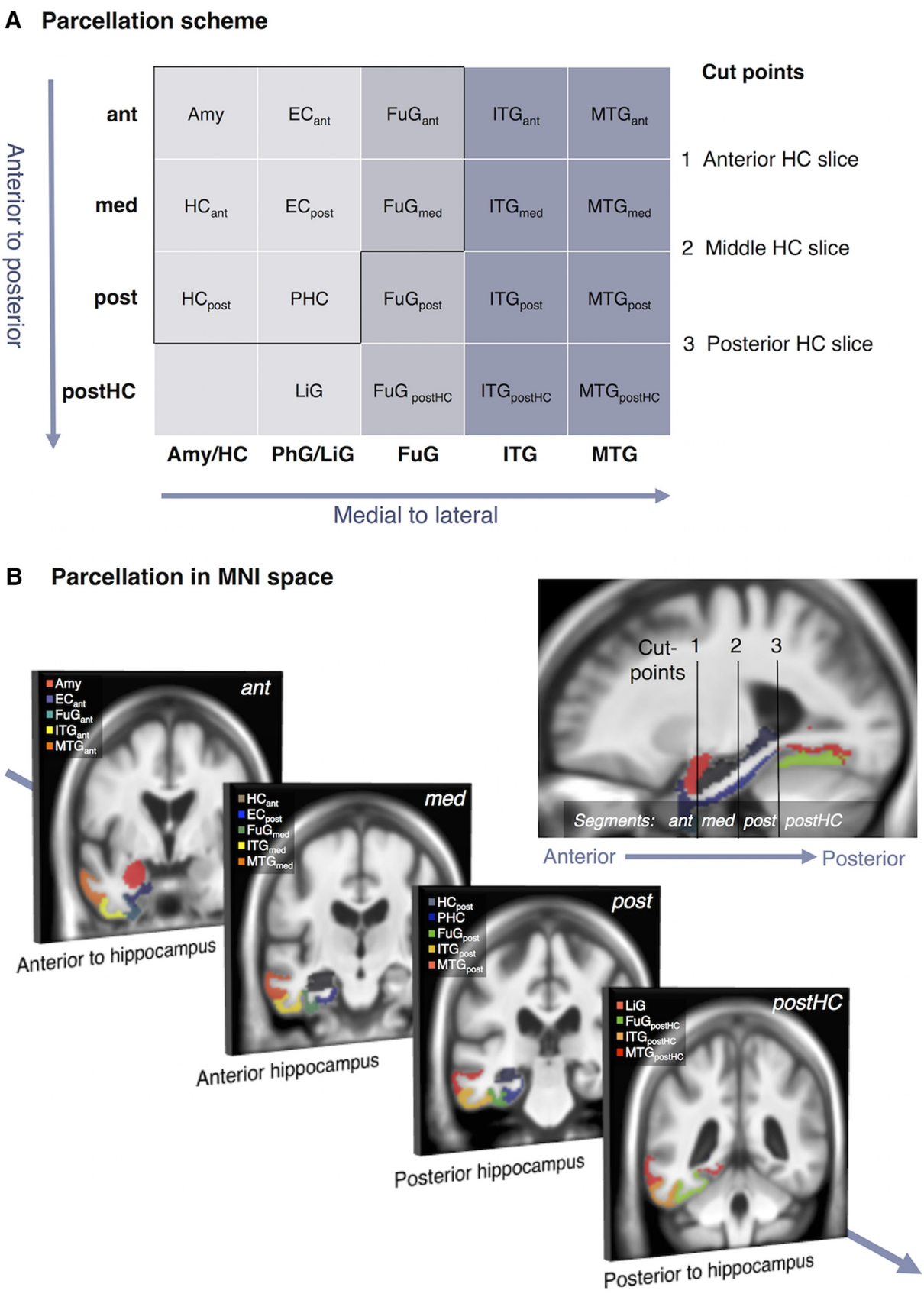

Figure 1. Temporal lobe parcellation. To assess subregional tau patterns measured by AV-1451 tau-tracer uptake in the temporal lobe, slicing was performed at three landmarks (cut points 1–3) across the longitudinal axis: at start, middle, and end of HC. This led to four segments (ant, med, post, postHC; y-axis in ***A***) of each gyrus (x-axis in ***A***). Note that only the med and post segments are equal in size. ***A***, The black outline highlights regions that compose the medial temporal lobe memory system. ***B***, The parcellation scheme is shown for the MNI group template (mean of normalized T1 images) but was also performed at individual (subject) level. Note that images are anterior commissure–posterior commissure aligned and not perpendicular to the long axis of the HC. Amy, Amygdala.

slice of the HC (counting all coronal HC slices and dividing by 2). The "post" segment ends on the last (most posterior) coronal slice of the HC, which also corresponds to the most posterior slice of the FreeSurfer defined "parahippocampal cortex." We called the part of FuG, ITG, and MTG posterior to the HC the "postHC." The PHC is posteriorly adjoined by the lingual gyrus (LiG). Our PhG_{ant} segment covers the anterior portion of EC, whereas our PhG_{med} segment covers the posterior portion of EC. The PhG_{post} segment corresponds to the PHC. Note that our boundary between the EC and PHC (middle of the HC) is more posterior than the FreeSurfer-defined landmark (end of amygdala), and approximately corresponded to the end of the HC head. We also note that BA36 or the lateral part of the perirhinal cortex is covered by the FuG, in particular the FuG_{ant} and FuG_{med}. We also assessed mean SUVRs from the amygdala, which borders the HC anteriorly. Temporal lobe subregional SUVRs were derived in individual (i.e., subject) space after the PVC but the same parcellation was also performed in MNI space without the PVC. Note that individual T1 images were coregistered and resliced (before parcellation) to the SPM-provided avg152T1.nii, which is anterior commissure–posterior commissure aligned.

AV-1451 data processing for analyses in MNI space. For voxelwise analyses, SUVR images (unsmoothed) were transformed into MNI152 space using DARTEL (diffeomorphic anatomical registration through exponentiated lie algebra). T1 images were segmented in SPM12. Native and DARTEL-imported gray and white matter segments were used to create a study-specific DARTEL template. The resulting flow fields served to normalize the SUVR images and the T1 images to MNI space (preserve concentration; resolution: $1.5 \times 1.5 \times 1.5\ mm^3$, no additional smoothing). We created a study-specific T1 group image by averaging across all warped T1 images. Similar to processing of T1 images in individual space, we segmented the T1-group image by FreeSurfer (Desikan–Killiany atlas) to derive ROIs that were used for the temporal lobe parcellation in MNI space (Figure 1*B*).

Experimental design and statistical analysis

ROI-based correlational analyses and regression models. First, we performed correlational analyses to describe the relationship between each cognitive measure and age, global PiB DVR, regional AV-1451 SUVR in Braak composite ROIs, bilateral entorhinal thickness, and bilateral HC volumes. Skipped Pearson correlation coefficients were obtained using the Robust Correlation Toolbox in Matlab (http://sourceforge.net/projects/robustcorrtool/) to limit the influence of outliers and data heteroscedasticity (Wilcox, 2004; Pernet et al., 2012). The toolbox (function skipped_correlation.m) performs Pearson tests after removing bivariate outliers by taking into account the overall structure of the data and provides bootstrapped 95% confidence intervals (CIs). Figures depict outliers excluded from the skipped Pearson correlation in black. Correlations were considered significant if the 95% CI did not include zero. These correlational analyses were only descriptive and not corrected for multiple comparisons (note that we performed a stepwise regression to identify the best predictor for episodic memory). The toolbox does not allow users to control for the effects of additional covariates, such as gender or education. However, education was not significantly related to any cognitive score (Pearson correlation, all p's ≥ 0.37, all r's ≤ 0.10). Gender was only related to the verbal memory score (which was not the major focus of this study) with female subjects performing better than males ($t_{(81)} = -2.9$, $p = 0.004$, independent sample t test).

We performed stepwise linear regressions in SPSS (IBM, V24) to identify which set of variables best predicted episodic-memory performance. We further ran general linear models (GLMs) to test for an interactive effect of $Braak_{I/II}$ AV-1451 SUVR, which was the best predictor of memory, and global Aβ [defined as continuous variable (i.e., PiB DVR) or categorically (i.e., PiB^+/PiB^-)] on episodic memory. We refrained from including age, gender, or education as covariates in our GLMs as these variables did not account for additional variance in the stepwise regression on episodic memory. Robust correlational analyses and GLMs were also used test how PiB DVR and age related to $Braak_{I/II}$ AV-1451 SUVR.

We further evaluated the local, regional specificity of memory–tau associations within the temporal lobe. Robust correlational analyses were performed between episodic memory performance and AV-1451 SUVR in 19 temporal lobe subregions in individual space (after PVC) and MNI space (without PVC). We derived bootstrapped 99.7% CIs (95% CI adjusted for 19 comparisons). Absolute skipped Pearson correlation coefficients are reported as heat maps.

We finally assessed the relationship of entorhinal-thickness change to temporal lobe tau measures and episodic-memory change in a subgroup of 57 OAs with longitudinal MRI and cognitive data by means of robust correlations.

When comparing the strength between robust dependent correlations, we used a percentile bootstrapping approach as described by Wilcox (2016). A Matlab script implementing the procedure is available on-line (https://github.com/GRousselet/blog/tree/master/comp2dcorr).

Voxelwise regressions. We performed voxelwise regressions in MNI space (without PVC) to further examine the spatial pattern of episodic memory–tau associations in the whole brain. The MNI-warped AV-1451 SUVR images were entered into a multiple-regression analysis in SPM12. We did not apply any explicit masking. Results are familywise error (FWE) corrected at cluster level ($p < 0.05$) with an uncorrected threshold of $p < 0.001$ at voxel level.

Linear mixed-effects models to derive slopes. To assess changes in entorhinal-thickness or episodic-memory performance over time, slopes were generated using a linear mixed-effects model in R ("lme4"). Entorhinal-thickness measures were derived by the longitudinal FreeSurfer pipeline. The following model, including random slopes and random intercepts, was fitted to the data, assuming that slopes and intercepts are independent: lmer[memory ~time + (time − 1 | Subj) + (1 | Subj)], where time is the time of the MRI scan or cognitive session in years relative to the first MRI or first session, respectively. The following model with correlated slopes and intercepts revealed very similar results: [lmer(memory ~ time + (1 + time | Subj)].

Results

Subject characteristics

The current sample included 83 cognitively normal OAs (age, 77 ± 6 years), of whom 36 were Aβ-positive ($A\beta^+$; PiB DVR, >1.065). Sample characteristics for the whole group as well as for Aβ-negative ($A\beta^-$) and $A\beta^+$ subjects separately are summarized in Table 1.

$A\beta^+$ subjects had significantly less education (16 ± 2 years) than $A\beta^-$ subjects (17 ± 2 years; $t_{(81)} = -2.34$, $p = 0.022$, independent samples t test) but did not differ in age, gender, or any structural measure (all p's ≥ 0.88). However, we note that the age range was broader in the $A\beta^-$ (60–93 years) than the $A\beta^+$ (69–86 years) subjects. The proportion of carriers of the apolipoprotein E (*APOE*) $\varepsilon 4$ allele was significantly higher in the $A\beta^+$ group [$\chi^2(1, N = 75) = 19.53$, $p < 0.001$, χ^2 test].

We created composite Z scores for episodic memory, comprising short-delay and long-delay free recall in a verbal and a visual memory task, as well as for working-memory and executive-function domains (see Materials and Methods). $A\beta^+$ and $A\beta^-$ subjects performed similarly for all composite scores (all t's ≤ 1.65, all p's ≥ 0.10, independent sample t test). $A\beta^+$ subjects performed worse on the CVLT short-delay free-recall test ($t_{(81)} = -1.99$, $p = 0.049$).

We also classified subjects into one of four stages based on AV-1451 SUVRs in composite ROIs that correspond to anatomical definitions of Braak stages I/II (transentorhinal), III/IV (limbic), and V/VI (neocortical; Schöll et al., 2016; Maass et al., 2017). Of 47 $A\beta^-$ subjects, 13 were assigned to stage 0, 31 to stage I/II, and only 3 to stage III/IV. In the $A\beta^+$ group, 5 of 36 subjects were classified as stage 0, 20 as stage I/II, and 11 as stage III/IV. No OA was assigned to stage V/VI. We thus constricted our subsequent analyses on associations with Braak ROI-based mean SUVR to $Braak_{I/II}$ and $Braak_{III/IV}$ composite ROIs.

Table 2. Correlation coefficients (95% CI) for associations of cognition with age, global Aβ PET, regional tau PET, and structural measures

	Age	Global Aβ	Braak$_{I/II}$ tau	Braak$_{III/IV}$ tau	Entorhinal thickness	HC volume
Episodic Memory	−0.10 [−0.31, 0.14]	−0.07 [−0.23, 0.09]	−0.35* [−0.50, −0.17]	−0.27* [−0.41, −0.12]	0.09 [−0.13, 0.32]	0.24* [0.01, 0.43]
Verbal memory	−0.13 [−0.33, 0.08]	−0.07 [−0.24, 0.10]	−0.25* [−0.43, −0.07]	−0.27* [−0.44, −0.08]	0.10 [−0.10, 0.31]	0.16 [−0.04, 0.35]
Visual memory	−0.12 [−0.30, 0.07]	−0.03 [−0.24, 0.17]	−0.38* [−0.53, −0.20]	−0.31* [−0.51, −0.11]	0.13 [−0.07, 0.33]	0.23* [0.02, 0.39]
Executive function	−0.10 [−0.29, 0.09]	−0.01 [−0.21, 0.21]	−0.22 [−0.41, 0.00]	−0.03 [−0.23, 0.17]	0.21* [0.01, 39]	0.14 [−0.06, 0.33]
Working memory	−0.01 [−0.23, 0.21]	−0.05 [−0.23, 0.16]	−0.15 [−0.34, 0.05]	−0.07 [−0.26, 0.14]	−0.13 [−37, 0.09]	0.06 [−0.13, 0.23]

Skipped Pearson correlation coefficients and bootstrapped 95% CIs derived from robust correlations (Pernet et al., 2012) across 83 OAs. Asterisks highlight significant correlations where the CI does not contain 0. Episodic memory was measured as a composite *Z* score of verbal and visual recall. Global Aβ was measured as PiB DVR in cortical regions. Tau was assessed by AV-1451 uptake in composite regions that approximate Braak stages (data are PV corrected). Bilateral (left and right averaged) HC volume and entorhinal thickness were derived by FreeSurfer segmentation from the MRI closest to the tau PET scan. HC volumes were adjusted for ICV.

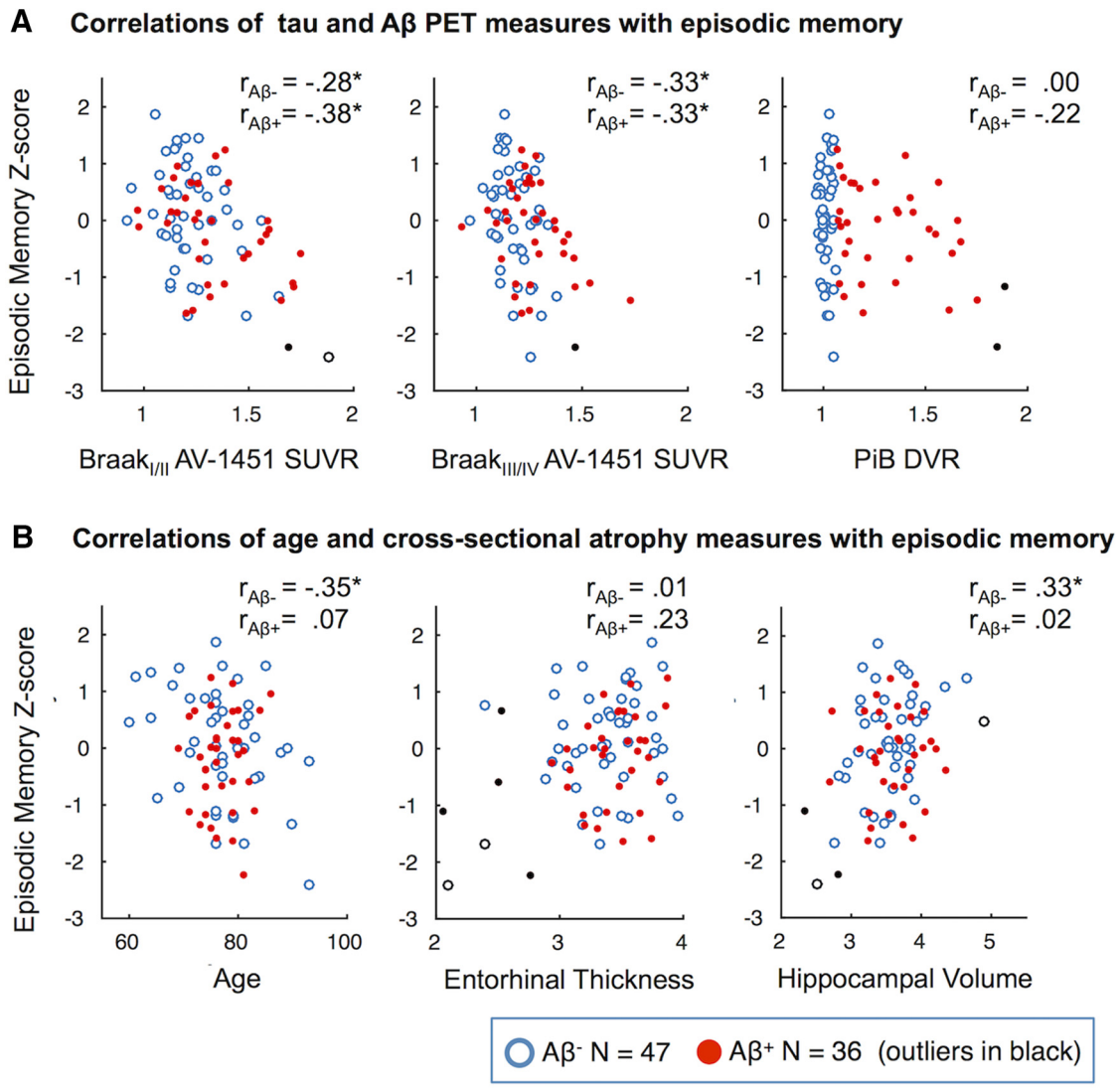

Figure 2. Relationships of tau, Aβ, age, and structural measures to episodic memory. Skipped Pearson correlation coefficients (*r*) and bootstrapped 95% CI were derived by robust correlations. Colors indicate Aβ status defined by PiB DVR (Aβ^- ≤1.065; Aβ^+ >1.065). Bivariate outliers excluded from the correlation are colored black. Asterisks highlight significant correlations where the bootstrapped 95% CI of *r* does not include zero. Episodic memory was measured as a composite *Z* score of verbal and visual recall. ***A***, Tau was assessed by AV-1451 uptake in composite regions that approximate Braak stages (after PVC). Global Aβ was measured as PiB DVR in cortical regions. ***B***, Bilateral mean HC volume (cm^3) and entorhinal thickness (cm^2) were derived by FreeSurfer segmentation from the MRI closest to the tau PET scan. HC volumes are adjusted for ICV.

Associations of age, Aβ, tau, and cross-sectional atrophy measures with cognition

First we performed correlational analyses to describe associations of age, global Aβ burden (PiB DVR), regional tau burden (bilateral mean AV-1451 SUVRs after PVC in Braak composite ROIs), and cross-sectional measures of MTL atrophy (HC volume, entorhinal thickness) with cognition. HC volumes were adjusted by ICV. Skipped Pearson correlation coefficients were derived by robust correlations (see Materials and Methods) and bootstrapped 95% CIs for correlations across all subjects are summarized in Table 2. Scatterplots with individual data color-coded by Aβ status as well as group-specific skipped Pearson correlation coefficients are shown in Figure 2. Data points (bivariate outliers) excluded ("skipped") from the correlation are shown in black. Robust correlations across all subjects revealed significant associations between the episodic memory composite score and AV-1451 SUVR, with

decreasing correlation strength from early MTL regions to limbic regions ($Braak_{I/II}$ $r = -0.35$ [−0.50, −0.17]; $Braak_{III/IV}$ $r = -0.27$ [−0.41, −0.12]). These correlations were significant for both $A\beta^-$ subjects ($Braak_{I/II}$ $r = -0.28$ [−0.50, −0.01]) and $A\beta^+$ subjects ($Braak_{I/II}$ $r = -0.38$ [−0.60, −0.15]; Fig. 2*A*). Of note, the relationship between episodic memory and AV-1451 SUVR in Braak ROIs was not hemisphere-specific and significant for both left and right side (all r's ≤ -0.28).

Robust correlations did not reveal a significant association between PiB DVR and episodic memory ($r = -0.07$, [−0.23, 0.09]) in either $A\beta^-$ ($r = -0.00$, [−0.27, 0.29]) or $A\beta^+$ subjects ($r = -0.22$, [−0.52, 0.13]; Fig. 2*A*). Associations of episodic memory with age and entorhinal thickness across all subjects were not significant (see Table 2 for CIs; Fig. 2*B*). If subjects were divided by Aβ status, age was related to memory in the $A\beta^-$ subjects ($r = -0.35$ [−0.58, −0.07]) but not the $A\beta^+$ subjects ($r = 0.07$ [−0.27, 0.41]). HC volume was positively related to episodic-memory performance across all subjects ($r = 0.24$ [0.01, 0.43]) and in $A\beta^-$ subjects ($r = 0.33$ [0.07, 0.54]), but not in $A\beta^+$ subjects ($r = 0.02$ [−0.26, 0.31]).

We also assessed correlations between episodic memory and tau-tracer uptake separately for visual (spatial figure) and verbal (word list) recall memory (Table 2). Verbal memory showed significant associations with AV-1451 SUVR in both Braak composite ROIs ($Braak_{I/II}$ $r = -0.25$ [−0.43, −0.07], $Braak_{III/IV}$ $r = -0.27$ [−0.44, −0.08]) but with none of the other variables. We note that there was also no significant relationship between verbal episodic-memory and volume or thickness measures when these were assessed separately for left and right hemisphere, although correlation strength was higher for the left side (EC: $r_{left} = 0.19$ [−0.02, 0.40]; $r_{right} = 0.02$ [−0.18, 0.23]; HC: $r_{left} = 0.20$ [−0.01, 0.40]; $r_{right} = 0.05$ [−0.18, 0.25]). Visual memory was also related to AV-1451 SUVR in all Braak ROIs ($Braak_{I/II}$ $r = -0.38$ [−0.53, −0.20], $Braak_{III/IV}$ $r = -0.31$ [−0.51, −0.11]) as well as to HC volume ($r = 0.23$ [0.02, 0.39]). The relationship between visual memory and HC volume was most robust if volumes were averaged across hemispheres ($r_{left} = 0.17$ [−0.04, 0.36], $r_{right} = 0.19$ [−0.02, 0.36]).

To assess the specificity of the relationship between tau-tracer uptake and episodic memory in our population, we also examined associations with executive function and working memory. The executive-function composite score was not significantly related to AV-1451 SUVR in any Braak ROI (Table 2) in either the $A\beta^+$ or in the $A\beta^-$ subjects. Also, working memory did not show a significant relationship with tau-tracer uptake in any Braak ROI (Table 2) in any of the groups. For associations of executive function or working memory with age, PiB DVR, and MRI measures, see also Table 2.

$Braak_{I/II}$ tau is the best predictor of memory

We performed stepwise linear regression analyses to identify which set of variables best predicted episodic memory in our elderly participants. Our set of predictors included age, PiB DVR, AV-1451 SUVR in $Braak_{I/II}$ and $Braak_{III/IV}$ ROIs, HC volume, and entorhinal thickness. $Braak_{I/II}$ SUVR was the best predictor of episodic memory ($F_{(1,81)} = 20.8$, $r^2_{adj} = 0.194$, $p < 0.001$, ANOVA; Model 1 in Table 3) with no other variable significantly improving the model. The only other variable that was marginally significant was HC volume ($t_{(81)} = 1.7$, $p = 0.09$), which may share variance with AV-1451 SUVRs for a number of reasons, including PVC. Other demographic variables, such as gender ($t_{(81)} = 1.49$, $p = 0.14$) or education ($t_{(81)} = 0.61$, $p = 0.54$), also did not significantly account for additional variance.

Table 3. GLMs predicting episodic memory by tau, Aβ, and their interaction

Model	$r^2_{adj.}/p$	Predictors	*B*	SE	*p*	Partial η^2
1.	0.19/<0.001	$Braak_{I/II}$ tau	−2.11	0.46	<0.001	0.20
		$Braak_{I/II}$ tau	−1.91	0.53	<0.001	0.14
2.	0.19/<0.001	Global Aβ	−0.36	0.46	0.44	0.01
		$Braak_{I/II}$ tau	−2.31	2.32	0.32	0.01
		Global Aβ	−0.85	2.81	0.77	0.00
3.	0.18/<0.001	Tau*Aβ	0.34	1.91	0.86	0.00

Episodic memory was measured as a composite *Z* score of verbal and visual recall. $Braak_{I/II}$ tau was measured by AV-1451 SUVR in the EC and HC (data are PV corrected); global Aβ was measured as PiB DVR across cortical regions.

We then ran GLMs to test whether there was an interaction effect between Aβ and $Braak_{I/II}$ tau on episodic memory (Table 3). In a model that only included main effects of both biomarkers (Model 2., $F_{(2,80)} = 10.6$, $r^2_{adj} = 0.190$, $p < 0.001$, ANOVA), $Braak_{I/II}$ SUVR significantly predicted memory ($B = -1.91$, SE = 0.53, $p < 0.001$) even when accounting for PiB DVR ($B = -0.36$, SE = 0.46, $p = 0.44$). In a model that comprised $Braak_{I/II}$ SUVR, PiB DVR and their interaction term (Model 3., $F_{(3,79)} = 7.0$, $r^2_{adj} = 0.180$, $p < 0.001$, ANOVA), the interaction was not significant ($B = 0.34$, SE = 1.91, $p = 0.86$). We note that there was also no evidence for an interaction between Aβ and $Braak_{I/II}$ tau on episodic memory when Aβ was defined as a categorical variable (interaction: $B = -0.57$, SE = 0.97, $p = 0.56$; Aβ: $B = 0.83$, SE = 1.27, $p = 0.52$; $Braak_{I/II}$ SUVR: $B = -1.78$, SE = 0.66, $p < 0.001$). This is also reflected by the finding that the slopes for the linear regression of memory on $Braak_{I/II}$ SUVR were similar between $A\beta^-$ subjects (slope = −2.35, $r^2 = 0.18$, $F_{(1,45)} = 9.97$, $p = 0.003$) and $A\beta^+$ subjects (slope = −1.78, $r^2 = 0.19$, $F_{(1,34)} = 8.21$, $p = 0.007$). We note that results were consistent when using non-PV-corrected $Braak_{I/II}$ mean SUVRs.

Age and Aβ independently predict increased $Braak_{I/II}$ tau

We further tested how global Aβ and age were related to tau-tracer uptake in $Braak_{I/II}$ and $Braak_{III/IV}$ ROIs. The association between PiB DVR and AV-1451 SUVR in $Braak_{I/II}$ and $Braak_{III/IV}$ composite ROIs is illustrated in Figure 3*A*. In $A\beta^+$ subjects, higher PiB DVR was related to higher AV-1451 SUVR in $Braak_{I/II}$ ROIs ($r = 0.51$ [0.23, 0.73]), whereas the association did not reach significance in $Braak_{III/IV}$ ROIs using robust correlations ($r = 0.32$ [−0.01, 0.62]). In $A\beta^-$ subjects, there was no significant relationship between PiB DVR and AV-1451 SUVR in any Braak ROI ($Braak_{I/II}$ $r = 0.05$ [−0.24, 0.36]; $Braak_{III/IV}$ $r = 0.11$ [−0.17, 0.39]). The association between age and AV-1451 SUVR in $Braak_{I/II}$ and $Braak_{III/IV}$ composite ROIs is illustrated in Figure 3*B*. In $A\beta^-$ subjects, higher age was related to higher AV-1451 SUVR in $Braak_{I/II}$ ROIs ($r = 0.40$ [0.06, 0.63]), but not in $Braak_{III/IV}$ ROIs ($r = 0.23$ [−0.06, 0.51]). There was no significant relationship between age and AV-1451 SUVRs in $A\beta^+$ subjects ($Braak_{I/II}$ $r = 0.00$ [−0.30, 0.33]; $Braak_{III/IV}$ $r = 0.07$ [−0.26, 0.42]), but we note again that the age range was smaller in this group (69–86 years).

GLMs showed that both PiB DVR and age were significant (independent) predictors for $Braak_{I/II}$ SUVR ($F_{(2,80)} = 16.2$, $r^2_{adj} = 0.27$, $p < 0.001$, ANOVA; PiB DVR: $B = 0.42$, SE = 0.08, $p < 0.001$; age: $B = 0.01$, SE = 0.003, $p = 0.01$), although the effect size for age was small (Table 4). To summarize at this point, episodic memory was best predicted by $Braak_{I/II}$ SUVR, which increased with both higher age and higher PiB DVR. Notably, the two PiB^- subjects with the highest SUVR in $Braak_{I/II}$ regions and the lowest episodic-memory score were both >90 years old.

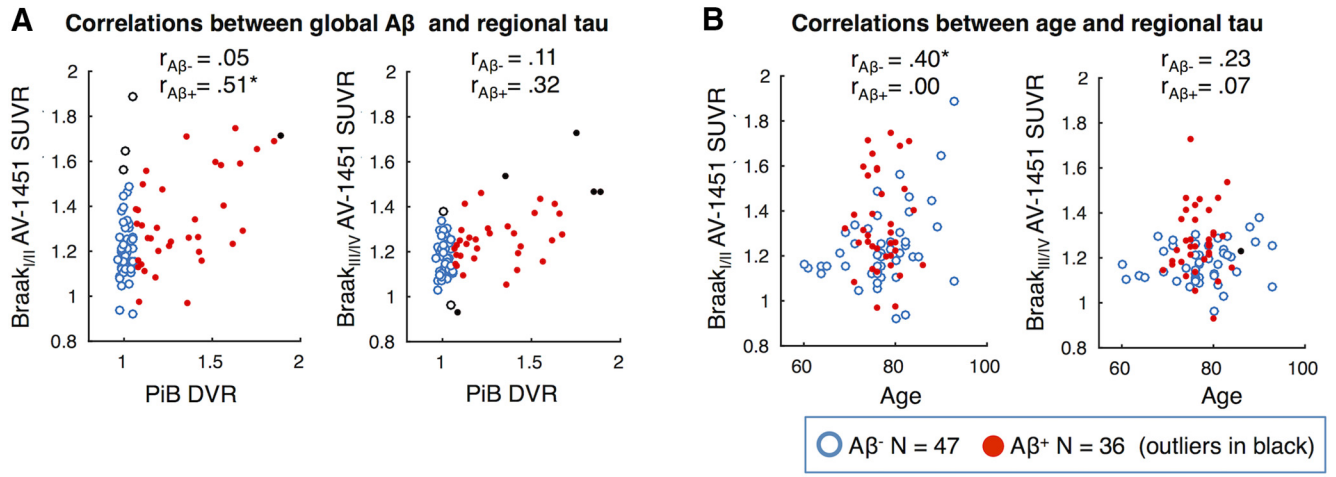

Figure 3. Relationships of Aβ (***A***) and age (***B***) to regional tau measures. Skipped Pearson correlation coefficients (r) and bootstrapped 95% CI were derived by robust correlations. Colors indicate Aβ status defined by PiB DVR (Aβ^-, ≤1.065; Aβ^+, >1.065). Bivariate outliers excluded from the correlation are colored in black. Asterisks highlight significant correlations where the bootstrapped 95% CI of r does not include zero. Tau was assessed by AV-1451 uptake in composite regions that approximate Braak stages (after PVC).

Table 4. GLMs predicting Braak$_{I/II}$ tau by global Aβ and age

Model	$r^2_{adj.}/p$	Predictors	*B*	SE	*p*	Partial η^2
1.	0.22/<0.001	Global Aβ	0.42	0.09	<0.001	0.23
		Global Aβ	0.42.	0.08	<0.001	0.25
2.	0.27/<0.001	Age	0.01	0.003	0.01	0.08
		Global Aβ	0.44	1.76	0.80	<0.01
		Age	0.01	0.02	0.74	<0.01
3.	0.26/<0.001	Aβ*age	<0.01	0.02	0.99	<0.01

Braak$_{I/II}$ tau was measured by AV-1451 SUVR in the EC and HC (data are PV corrected); global Aβ was measured as PiB DVR across cortical regions.

Entorhinal tau shows strongest relationship to episodic memory

ROI-based analyses on temporal lobe tau associations with memory

To examine local associations between temporal lobe tau-tracer uptake and memory, we used the FreeSurfer-derived ROIs of the HC, EC, PHC, FuG, ITG, and MTG (Desikan et al., 2006) and subdivided those along the longitudinal axis of the temporal lobe. The parcellation is schematically illustrated in Figure 1*A* and subregions are shown for the group T1 template in MNI space in Figure 1*B*. We used the most anterior, the middle, and the most posterior HC slice (Fig. 2, cut points 1–3) as landmarks to coronally slice each gyrus (PhG, FuG, ITG, MTG) into four segments (ant, med, post, postHC). A detailed description of the parcellation and labeling (which partly differs from FreeSurfer) is given in the Materials and Methods section. Note that we merged FreeSurfer EC and PHC ROIs before parcellation to derive a continuous PhG ROI. Our PhG$_{ant}$ and PhG$_{med}$ segments correspond to the anterior and posterior EC, respectively, whereas the PhG$_{post}$ segment corresponds to the PHC. We ran robust correlational analyses between memory performance and bilateral (i.e., left and right hemisphere averaged) AV-1451 SUVR values derived from each temporal lobe subregion in subject space after PVC and in MNI space (CIs adjusted for multiple comparisons).

Absolute skipped Pearson correlation coefficients for the association between temporal lobe SUVRs derived from subject space and episodic memory are displayed as a heat map in Figure 4*A*. Episodic-memory composite scores were significantly associated with AV-1451 SUVRs in all PhG regions, comprising anterior EC (=PhG$_{ant}$, $r = -0.39$ [−0.63, −0.10]), posterior EC (=PhG$_{med}$, $r = -0.41$ [−0.62, −0.14]), and PHC (=PhG$_{post}$, $r = -0.37$ [−0.60, −0.10]). Furthermore, the correlation was significant with the posterior FuG (FuG$_{post}$, $r = -0.37$ [−0.63, −0.08]). Notably, the LiG, which joins the PhG posteriorly, did not show a significant correlation with memory ($r = -0.18$, [−0.45, 0.04]). Scatterplots for the association between memory and all three segments of the PhG as well as the LiG are illustrated in Figure 4*B*. Associations between tau-tracer uptake in PhG subregions and episodic memory were significant in both Aβ^- and Aβ^+ subjects (Fig. 4*B*).

The non-PV-corrected MNI space data revealed a similar pattern with the strongest correlation between episodic memory and tau-tracer uptake found with the posterior EC ($r = -0.43$ [−0.67, −0.14]; all other r's ≥ −0.36; data not shown).

Moreover, these findings were consistent across modalities with the posterior EC SUVR showing strongest associations with verbal recall memory ($r = -0.37$ [−0.60, −0.08], all other r's ≥ −0.33) and visual memory ($r = -0.50$ [−0.69, −0.26], all other r's ≥ −0.32) compared with other temporal lobe regions. This is shown in Figure 4*C*.

The ITG is a region of particular interest, as it shows strong differences in tau PET signal between AD patients and controls (for review, see Saint-Aubert et al., 2017). We compared the association between episodic memory and AV-1451 mean SUVR in EC versus ITG by means of a percentile bootstrapping approach (Wilcox, 2016; see Material and Methods). We found that the correlation of episodic memory with the EC was significantly stronger than with the ITG mean SUVR ($\Delta r = -0.13$ [−0.24 −0.02], $p = 0.02$, one-sided $\alpha = 0.05$).

Whole-brain voxelwise analyses on tau–memory associations

We also performed voxelwise regressions in MNI space to further examine the spatial pattern of memory–tau associations in the whole brain and to confirm our ROI-based findings. Predicting episodic memory by AV-1451 tau-tracer uptake revealed four significant clusters, all located in the medial or lateral temporal lobe ($p_{cluster(FWE)} < 0.05$, $p_{voxel(uncorr)} < 0.001$, no explicit mask). The global maximum was located in the left lateral EC at the transition toward the perirhinal cortex at the rostrocaudal level of the anterior HC head (Fig. 5, blue cross). The cluster covered the posterior EC as well as parts of anterior EC and PHC. The same

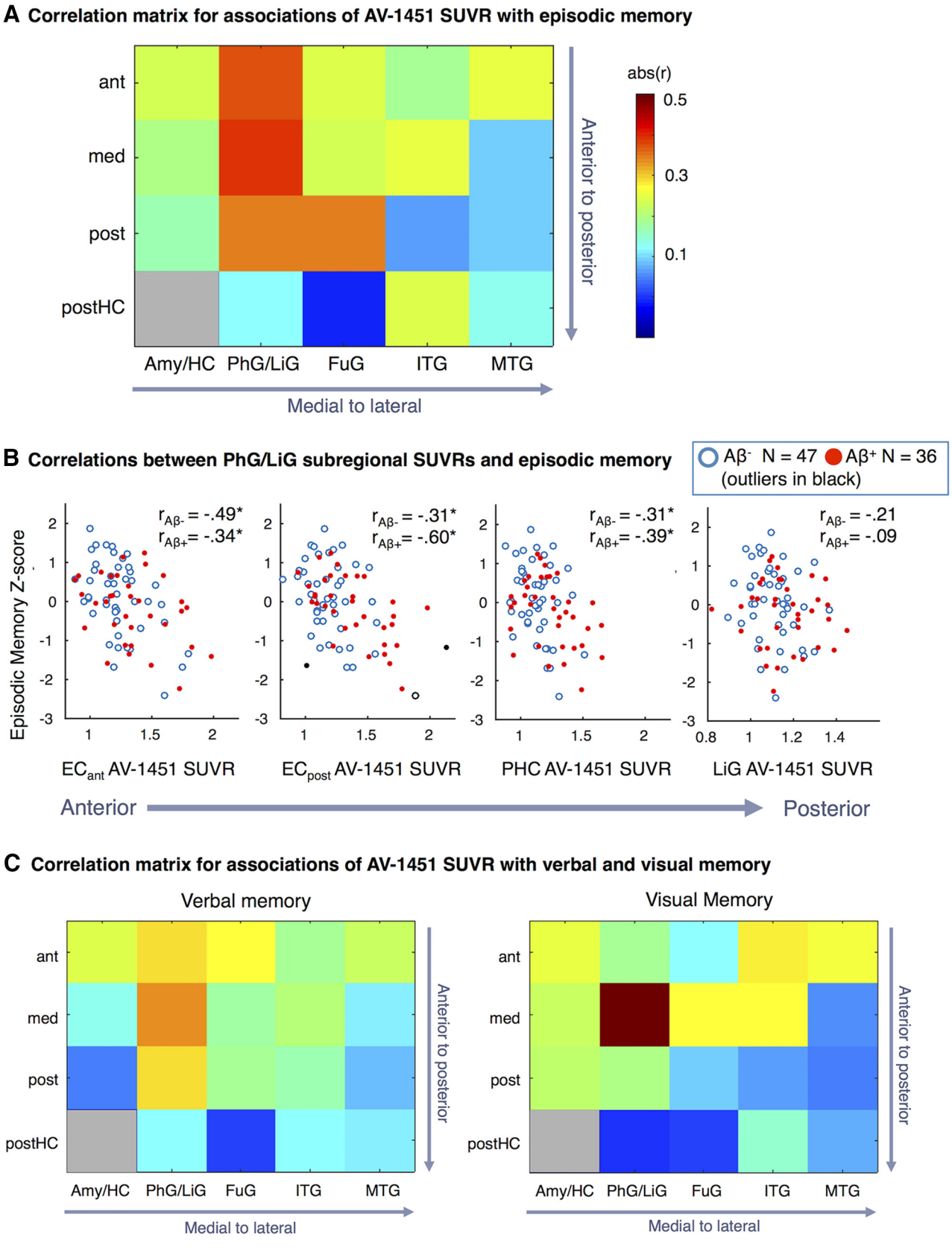

Figure 4. Relationships between memory and temporal lobe regional tau PET measures. ***A***, Correlation matrix showing absolute skipped Pearson correlation coefficients for the association between bilateral AV-1451 mean SUVR in temporal lobe subregions and episodic memory ($n = 83$). Correlations were strongest with PhG, specifically PhG_{med} corresponding to the posterior EC. Parcellation was performed in subject space with PVC. ***B***, Correlation plots for PhG/LiG subregions from anterior to posterior: PhG_{ant} (= EC_{ant}), PhG_{med} (= EC_{post}), PhG_{post} (= PHC), and LiG. *R* values denote skipped Pearson correlation coefficients after exclusion of outliers, which are colored black. Asterisks highlight significant correlations where the bootstrapped 95% CI of *r* does not include zero. ***C***, Skipped Pearson correlations between bilateral SUVRs derived from individual space parcellation and verbal (left) versus visual (right) recall memory. Correlations were strongest in EC_{post} across modalities. The color bar in ***A*** also applies to ***C***.

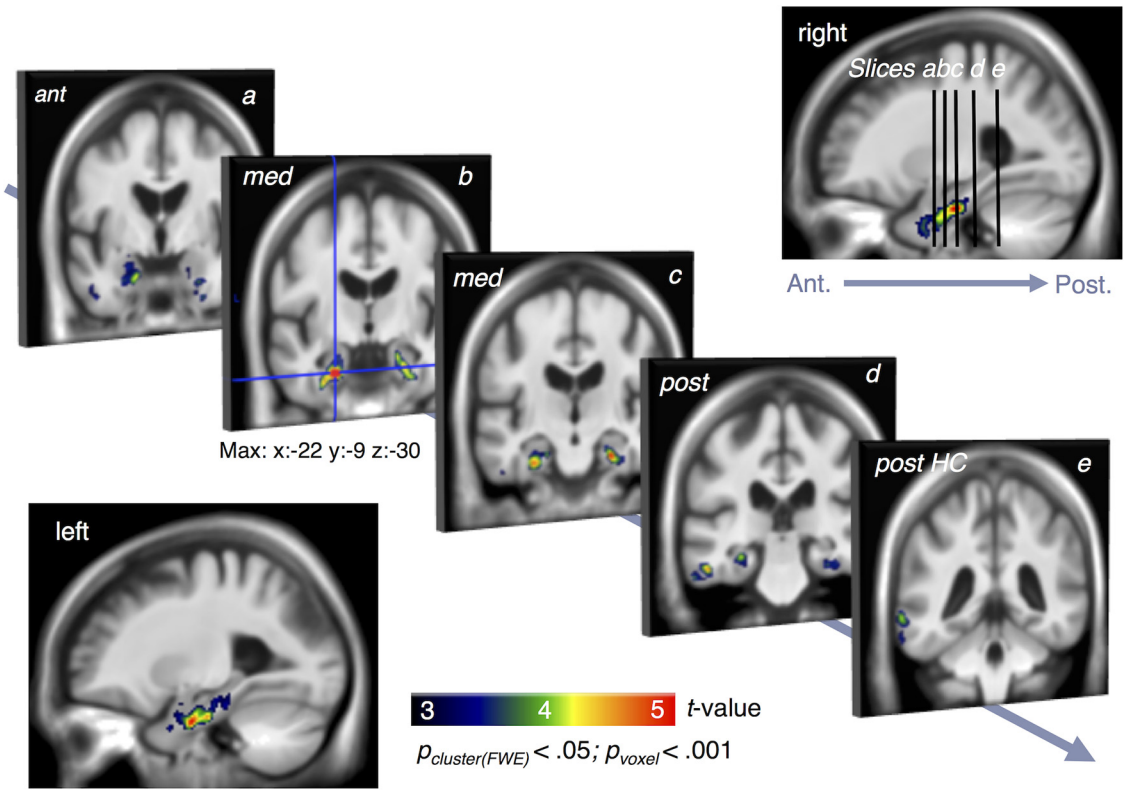

Figure 5. Voxelwise regressions of episodic memory on tau-tracer uptake (whole brain) in MNI space. AV-1451 SUVR significantly predicted episodic memory in four regions: left EC/PHC (global maximum in left transentorhinal region at level of anterior HC head; blue cross), right EC/PHC, left posterior ITG and posterior MTG. Results are FWE-corrected at cluster level ($p_{cluster} < 0.05$, $p_{voxel} < 0.001$). No explicit mask was used.

Table 5. Voxelwise regression results of AV-1451 SUVR on episodic memory

Region	Side	Cluster *p*(FWE-corrected)	Cluster size	Peak *T*	*x*, *y*, *z* (mm)
EC/PHC	left	<0.001	1387	5.57	−22 −9 −30
EC/PHC	right	0.001	1043	4.96	27 −16 −27
ITG	left	0.002	905	4.82	−52 −28 −21
MTG	left	0.036	557	4.46	−44 −62 18

Results are FWE-corrected at cluster level ($p_{cluster} < 0.05$, $p_{voxel} < 0.001$). No explicit mask was used.

region was significant on the right side. Furthermore, significant voxelwise relations were found with regions in left medial to posterior ITG and left posterior MTG. Peak coordinates are summarized in Table 5.

Entorhinal-thickness atrophy closely mirrors tau pathology

Fifty-seven of 83 OAs had longitudinal MRI as well as cognitive data (≥2 scans/testing sessions). Longitudinal MRI data comprised ≤5 scans over a period of 4.5 ± 2.6 years and an average delay of 2 years between scans. Longitudinal cognitive data comprised ≤10 sessions over a period of 5.6 ± 2.5 years and an average delay of 1 year between sessions. More details about the longitudinal data can be found in Materials and Methods. In this subsample, we assessed the relationship of entorhinal-thickness change with AV-1451 SUVR, PiB DVR, and episodic-memory change. We used all available MRI data and cognitive data to derive slopes by means of linear mixed-effects models. The AV-1451 tau scan was acquired between 2.7 years before to 0.7 years after the last MRI and similarly between 2.8 years before to 0.7 years after the last cognitive session. For 40% of subjects, the tau scan was acquired after or at the time of the last MRI scan, such that atrophy data were fully retrospective. Regarding the cognitive data, in 30% of subjects, measures of memory decline were fully retrospective to the tau scan.

We found that entorhinal-thickness changes were strongly correlated with $Braak_{I/II}$ SUVRs ($r = -0.60$ [−0.78, −0.36]; Fig. 6*A*), whereas the relationship with $Braak_{III/IV}$ ROIs was not significant ($r = -0.15$ [−0.38, 0.11]). Notably, entorhinal-atrophy measures were related to $Braak_{I/II}$ tau measures in both $A\beta^-$ ($r = -0.53$ [−0.82, −0.08], $n = 28$) and $A\beta^+$ subjects ($r = -0.64$ [−0.82, −0.34], $n = 29$). When using non-PV-corrected data, correlation strength was lower (OA: $r = -0.40$ [−0.63, −0.15]; $A\beta^-$: $r = -0.45$ [−0.80, 0.02]; $A\beta^+$: $r = -0.42$ [−0.69, −0.05]), although still significant across the whole group (data not shown). Global PiB DVR was not significantly related to entorhinal-thickness change ($r = -0.11$ [−0.33, 0.14]). Entorhinal-thickness change was also correlated with change in episodic memory ($r = 0.33$ [0.09, 0.54]; Fig. 6*A*). Similarly, $Braak_{I/II}$ SUVR was related to change in episodic memory ($r = -0.37$ [−0.55, −0.17]; Fig. 6*A*). We note that in accordance with our cross-sectional analyses on episodic-memory performance (Fig. 2*A*), change in memory was related to $Braak_{I/II}$ SUVRs in both $A\beta^-$ ($r = -0.41$ [−0.55, −0.17]) and $A\beta^+$ ($r = -0.61$ [−0.78, −0.29]) subjects.

Furthermore, we assessed the regional specificity of associations between EC atrophy or episodic-memory decline and temporal lobe tau PET tracer retention. A heat map displaying skipped Pearson coefficients across all temporal lobe subregions, derived by parcellation as described in the preceding text, is depicted in Figure 6*B*. Correlations between EC-thickness change and AV-1451 SUVR were only significant in the MTL ($r \leq -0.46$) including the PhG and HC subregions as well as amygdala (all other r's > -0.29). The correlation between EC-thickness change and AV-1451 SUVR was strongest in the posterior EC (PhG_{med}, $r = -0.58$

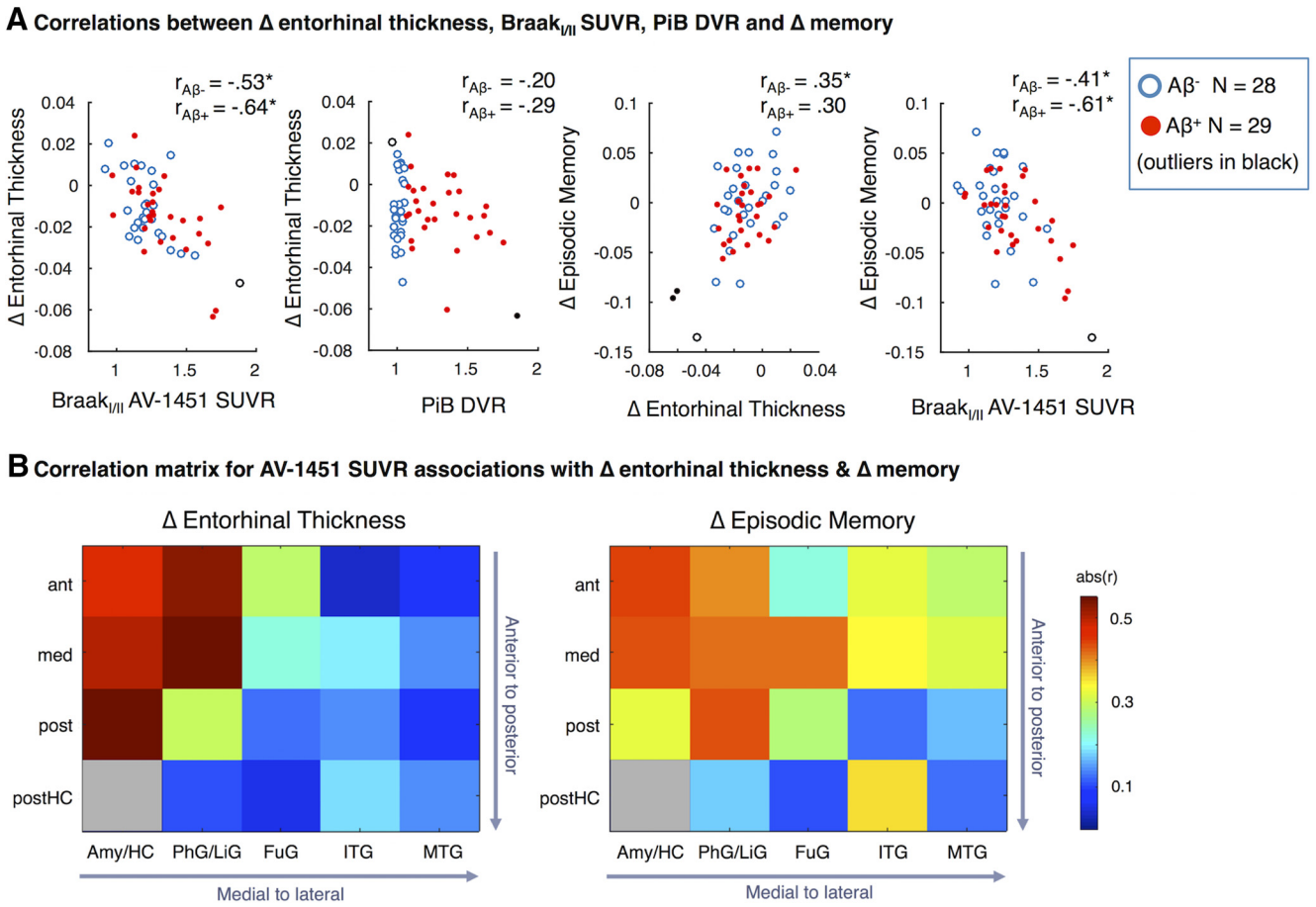

Figure 6. Relationship between entorhinal-thickness atrophy, tau, and Aβ PET measures, and episodic-memory decline. Longitudinal MRI data were available for 57 OAs and processed with the longitudinal FreeSurfer pipeline. The same subjects had longitudinal cognitive data. Bilateral mean entorhinal-thickness and episodic-memory changes were estimated by linear mixed-effects models. ***A***, Skipped Pearson correlation coefficients (r) and bootstrapped 95% CI were derived by robust correlations. Colors indicate Aβ status defined by PiB DVR (Aβ^-, $\leq$1.065; Aβ^+, $>$1.065). Asterisks highlight significant correlations where the bootstrapped 95% CI of r does not include zero. ***B***, Correlation matrix showing absolute skipped Pearson correlation coefficients for the association between bilateral AV-1451 mean SUVR in temporal lobe subregions and entorhinal-thickness change (left) and episodic-memory change (right).

[−0.75, −0.34]), the same region that showed strongest associations with episodic memory in the full sample (Fig. 4). Notably, this pattern of associations between entorhinal atrophy and tau measures being confined to MTL subregions was consistent when using non-PV-corrected SUVRs, although correlations were slightly weaker. Similarly, episodic-memory change was negatively related to AV-1451 SUVR in MTL regions ($r \leq -0.40$) including the PhG, amygdala, anterior HC, and FuG_{med} (ROI that includes the perirhinal cortex). The pattern of associations between temporal lobe tau-tracer retention and memory change was similar to cross-sectional associations (Fig. 4*A*) but with involvement of amygdala and HC in addition to the EC and PHC.

In summary, we found strong local associations between entorhinal-thickness atrophy and *in vivo* tau pathology, which closely mirrored the relationship between tau and cross-sectional as well as longitudinal measures of episodic memory.

Discussion

We investigated how age and *in vivo* measures of regional tau, global Aβ burden, and MTL atrophy contribute to episodic-memory performance in cognitively normal elderly. We found that tau-tracer uptake in $Braak_{I/II}$ regions comprising the EC and HC best explained episodic-memory performance, with no additional value from any other variable. There was no interaction of Aβ and $Braak_{I/II}$ tau on memory. Associations of tau tracer retention with episodic memory were strongest in the EC and present in subjects with and without evidence of Aβ accumulation. In Aβ^- subjects, higher MTL tau PET measures were related to older age. Furthermore, entorhinal tau measures were linked to entorhinal atrophy and episodic-memory decline in subjects with longitudinal MRI and cognitive data. Our findings are consistent with neuropathological data that showed a close relationship between NFTs in PhG and memory impairments across OAs and patients (Mitchell et al., 2002). Our data also extend previous results by showing that effects of tau on memory are independent of several additional variables, most notably Aβ, that there is regional specificity to this relationship, particularly involving the EC/transentorhinal cortex, and that tau deposition is related to longitudinal EC atrophy. Together, our data, obtained during life, suggest that entorhinal tau pathology and related atrophy underlie memory impairments typically seen in old age even in the absence of Aβ. These findings of an Aβ-independent/age-dependent tauopathy related to cognition are consistent with the concept of PART (Josephs et al., 2017; Crary et al., 2014).

Several previous PET studies in samples that included AD patients reported associations between episodic memory and tau-tracer uptake in the MTL, whereas global cognition was associated with tau in wider neocortical regions (Cho et al., 2016a; Ossenkoppele et al., 2016; Maass et al., 2017). Brier et al. (2016) studied

associations between tau and Aβ PET topographies and cognition in a sample of controls and mildly impaired patients. Their data revealed tau PET as the dominant topography contributing to episodic memory. However, they found that the tau topographies were sparse, comprising mostly temporal regions, for all domains except episodic memory, where the topography covered broader neocortical regions. In a small sample of 18 $A\beta^-$ OAs, Shimada et al. (2016) reported voxelwise associations (at an uncorrected threshold) between logical memory and ^{11}[C]PBB3 tau-tracer uptake in the HC and several cortical regions. Whether the relationship between memory and tau measures is constrained to the MTL or seen with wider neocortical areas is likely related to the sample, with patients that bear more widespread tau pathology and more severe memory impairments often driving associations.

Our temporal lobe parcellation revealed strongest associations between episodic memory and tau-tracer retention in the PhG, most prominently in the posterior EC. This was true across memory modalities. Voxelwise analyses confirmed these findings and showed that the peak for the memory–tau PET associations was located in the left lateral EC at the transition toward the perirhinal cortex at the rostrocaudal level of the anterior HC head. A similar area showed the strongest correlation on the right side. Braak and Braak defined the transentorhinal area on a section that included the HC at the uncal level and a full description of its anterior—posterior extent is lacking. Notably, our EC ROI also covered the medial bank of the collateral sulcus, and thus likely included the transentorhinal area. Due to the low resolution of our PET data (6–7 mm isotropic), we cannot dissociate lateral and medial parts of the PhG. Still it is striking that among all temporal lobe regions, the EC—the first cortical region where NFTs accumulate—was most strongly linked to episodic memory. This association was most prominent in the posterior part of EC, but also present in neighboring regions, such as the anterior EC and PHC. MRI studies with higher imaging resolution may shed more light on dysfunction or atrophy of entorhinal subregions (Maass et al., 2015; Olsen et al., 2017; e.g., anterolateral vs posteromedial) in relation to *in vivo* tau pathology.

The EC is a major cortical hub (Bota et al., 2015) that mediates HC-neocortical communication and is critical to memory formation. On the one hand, episodic-memory decline is one of the earliest cognitive signs of AD dementia and entorhinal atrophy is a sensitive marker that predicts the conversion from "normal aging" to AD (Killiany et al., 2002; Desikan et al., 2009). High-resolution MR imaging has shown the most significant volume and thickness differences between MCI patients and older controls in the left BA35, corresponding to the transentorhinal region (Yushkevich et al., 2015). The BA35 was also the only region where thickness measures discriminated $A\beta^+$ from $A\beta^-$ OAs (Wolk et al., 2017). Olsen et al. found reductions in anterolateral EC volume, including the transentorhinal area, in clinically normal OAs "at risk" for MCI due to low cognitive performance (2017). Evidence for early metabolic dysfunction in the lateral EC in preclinical AD is supported by diminished perfusion in those adults that progress to AD (Khan et al., 2014). On the other hand, transentorhinal tau pathology and decreased episodic-memory performance are common in clinically normal elderly. Fjell et al. (2014) found similar rates of entorhinal thinning in participants with very low probability of incipient AD compared with a bigger sample of OAs, and the changes were predictive of changes in memory. This suggested that EC thinning in advanced age, even in areas vulnerable to AD, can be part of a "normal" aging process.

Since tau pathology is age-related, accumulates early in the MTL, and relentlessly progresses in the course of AD (Braak and Braak, 1997), it is reasonable to assume that deterioration of memory function is present in both cognitively normal elderly and in AD dementia. In our study, high entorhinal tau measures, along with entorhinal atrophy, and low memory performance were present in subjects with and without Aβ (the latter being concordant with the concept of PART). Our data cannot unravel whether those individuals are on a path toward AD. In the current view, this transition is characterized by the spread of tau tangles outside the MTL, which seems to require the presence of Aβ, and leads to worsening of global cognition (Sperling et al., 2014).

Our data did not support any link between tau or Aβ PET measures either with working memory, confirming findings by Brier et al. (2016), or with executive function in normal elderly. This is in accordance with a meta-analysis that did not reveal evidence for associations between PiB measures and working memory or executive function in cognitively normal OAs (Hedden et al., 2013). Effects of Aβ and tau pathology on executive function or working memory may be profound in later stages of AD, when tau pathology has spread to Braak V areas. Within OAs without a diagnosis of dementia, gray and white matter degradation of frontal-striatal networks is thought to be the major cause underlying deficits in executive function (Buckner, 2004; Hedden and Gabrieli, 2004).

Regarding episodic memory, $Braak_{I/II}$ tau-tracer retention accounted for 20% of the variance in our data. Measures of MTL structure, Aβ burden, age, gender, or education did not explain additional variance in memory performance. In a neuropathological study on the contributions of Aβ load, NFT density, infarcts, and Lewy bodies to cognitive decline in OAs, only tangles accounted for episodic-memory decline when all pathologies were considered simultaneously (Boyle et al., 2013b). Furthermore, the pathologic indices of AD, cerebrovascular disease, and Lewy body disease together explained only 41% of the variance in global cognitive decline (Boyle et al., 2013a). Hedden and colleagues found that multiple *in vivo* brain markers (structural measures, white matter hyperintensities, fractional anisotropy, functional connectivity, and PET measures of glucose metabolism and Aβ) together accounted for 20% of variation in episodic memory. These data indicate that while many different variables underlie memory decline, a large proportion of late-life cognitive variance remains unexplained, even when neuropathological data are available. Other potential factors for age-related variability in memory function include changes in the dopaminergic system that primarily target frontal-striatal networks (Bäckman et al., 2010; Berry et al., 2016). Moreover, some individuals might show a higher ability to tolerate or respond to pathology, thereby minimizing its impact on cognition (concept of cognitive reserve; Arenaza-Urquijo et al., 2015).

To summarize, tau-tracer uptake in a region coinciding with the location of the transentorhinal cortex predicted episodic-memory performance in our cohort of cognitively normal OAs independent of Aβ status. Furthermore, tau measures and episodic-memory decline were tightly linked to entorhinal atrophy. Our data suggest that entorhinal tangle pathology is a major factor contributing to memory decline in old age. While Aβ might accelerate tau pathology within and initiate spread outside the MTL, it does not seem to underlie age-related memory decline. Longitudinal tau and Aβ PET data are necessary to better understand the causal and temporal link between both pathologies and to elucidate which factors predict the conversion toward AD.

References

Arenaza-Urquijo EM, Wirth M, Chételat G (2015) Cognitive reserve and lifestyle: moving towards preclinical Alzheimer's disease. Front Aging Neurosci 7:134. CrossRef Medline

Bäckman L, Lindenberger U, Li SC, Nyberg L (2010) Linking cognitive aging to alterations in dopamine neurotransmitter functioning: recent data and future avenues. Neurosci Biobehav Rev 34:670–677. CrossRef Medline

Baker SL, Maass A, Jagust WJ (2017a) Considerations and code for partial volume correcting [18F]-AV-1451 tau PET data. Data in Brief *15*, 648–657. CrossRef Medline

Baker SL, Lockhart SN, Price JC, He M, Huesman RH, Schonhaut D, Faria J, Rabinovici G, Jagust WJ (2017b) Reference tissue-based kinetic evaluation of 18F-AV-1451 in aging and dementia. J Nucl Med 52:332–338. CrossRef Medline

Bennett DA, Schneider JA, Wilson RS, Bienias JL, Arnold SE (2004) Neurofibrillary tangles mediate the association of amyloid load with clinical Alzheimer disease and level of cognitive function. Arch Neurol 61:378–384. CrossRef Medline

Berron D, Vieweg P, Hochkeppler A, Pluta JB, Ding SL, Maass A, Luther A, Xie L, Das SR, Wolk DA, Wolbers T, Yushkevich PA, Düzel E, Wisse LEM (2017) A protocol for manual segmentation of medial temporal lobe subregions in 7 tesla MRI. Neuroimage Clin 15:466–482. CrossRef Medline

Berry AS, Shah VD, Baker SL, Vogel JW, O'Neil JP, Janabi M, Schwimmer HD, Marks SM, Jagust WJ (2016) Aging affects dopaminergic neural mechanisms of cognitive flexibility. J Neurosci 36:12559–12569. CrossRef Medline

Bota M, Sporns O, Swanson LW (2015) Architecture of the cerebral cortical association connectome underlying cognition. Proc Natl Acad Sci U S A 112:E2093–E2101. CrossRef Medline

Boyle PA, Wilson RS, Yu L, Barr AM, Honer WG, Schneider JA, Bennett DA (2013a) Much of late life cognitive decline is not due to common neurodegenerative pathologies. Ann Neurol 74:478–489. CrossRef Medline

Boyle PA, Yu L, Wilson RS, Schneider JA, Bennett DA (2013b) Relation of neuropathology with cognitive decline among older persons without dementia. Front Aging Neurosci 5:50. CrossRef Medline

Braak H, Braak E (1985) On areas of transition between entorhinal allocortex and temporal isocortex in the human brain. Normal morphology and lamina-specific pathology in Alzheimer's disease. Acta Neuropathol 68:325–332. CrossRef Medline

Braak H, Braak E (1991) Neuropathological stageing of Alzheimer-related changes. Acta Neuropathol 82:239–259. CrossRef Medline

Braak H, Braak E (1997) Frequency of stages of Alzheimer-related lesions in different age categories. Neurobiol Aging 18:351–357. CrossRef Medline

Brier MR, Gordon B, Friedrichsen K, McCarthy J, Stern A, Christensen J, Owen C, Aldea P, Su Y, Hassenstab J, Cairns NJ, Holtzman DM, Fagan AM, Morris JC, Benzinger TL, Ances BM (2016) Tau and Aβ imaging, CSF measures, and cognition in Alzheimer's disease. Sci Transl Med 8:338ra66. CrossRef Medline

Buckner RL (2004) Memory and executive function in aging and AD: multiple factors that cause decline and reserve factors that compensate. Neuron 44:195–208. CrossRef Medline

Cho H, Choi JY, Hwang MS, Lee JH, Kim YJ, Lee HM, Lyoo CH, Ryu YH, Lee MS (2016a) Tau PET in Alzheimer disease and mild cognitive impairment. Neurology 87:375–383. CrossRef Medline

Cho H, Choi JY, Hwang MS, Kim YJ, Lee HM, Lee HS, Lee JH, Ryu YH, Lee MS, Lyoo CH (2016b) *In vivo* cortical spreading pattern of tau and amyloid in the Alzheimer disease spectrum. Ann Neurol 80:247–258. CrossRef Medline

Crary JF, Trojanowski JQ, Schneider JA, Abisambra JF, Abner EL, Alafuzoff I, Arnold SE, Attems J, Beach TG, Bigio EH, Cairns NJ, Dickson DW, Gearing M, Grinberg LT, Hof PR, Hyman BT, Jellinger K, Jicha GA, Kovacs GG, Knopman DS, et al. (2014) Primary age-related tauopathy (PART): a common pathology associated with human aging. Acta Neuropathol 128:755–766. CrossRef Medline

Delis DC, Kramer JH, Kaplan E, Ober BA (2000) California Verbal Learning Test-Second Edition San Antonio, TX: The Psychological Corporation.

Desikan RS, Ségonne F, Fischl B, Quinn BT, Dickerson BC, Blacker D, Buckner RL, Dale AM, Maguire RP, Hyman BT, Albert MS, Killiany RJ (2006) An automated labeling system for subdividing the human cerebral cortex on MRI scans into gyral-based regions of interest. Neuroimage 31:968–980. CrossRef Medline

Desikan RS, Cabral HJ, Hess CP, Dillon WP, Glastonbury CM, Weiner MW, Schmansky NJ, Greve DN, Salat DH, Buckner RL, Fischl B, Fischl B (2009) Automated MRI measures identify individuals with mild cognitive impairment and Alzheimer's disease. Brain 132:2048–2057. CrossRef Medline

Duyckaerts C, Braak H, Brion JP, Buée L, Del Tredici K, Goedert M, Halliday G, Neumann M, Spillantini MG, Tolnay M, Uchihara T (2015) PART is part of Alzheimer disease. Acta Neuropathol 129:749–756. CrossRef Medline

Fjell AM, Westlye LT, Grydeland H, Amlien I, Espeseth T, Reinvang I, Raz N, Dale AM, Walhovd KB, Walhovd KB (2014) Accelerating cortical thinning: unique to dementia or universal in aging? Cereb Cortex 24:919–934. CrossRef Medline

Folstein MF, Folstein SE, McHugh PR (1975) "Mini-mental state". A practical method for grading the cognitive state of patients for the clinician. J Psychiatr Res 12:189–198. Medline

Giannakopoulos P, Herrmann FR, Bussière T, Bouras C, Kövari E, Perl DP, Morrison JH, Gold G, Hof PR (2003) Tangle and neuron numbers, but not amyloid load, predict cognitive status in Alzheimer's disease. Neurology 60:1495–1500. CrossRef Medline

Hedden T, Gabrieli JD (2004) Insights into the ageing mind: a view from cognitive neuroscience. Nat Rev Neurosci 5:87–96. Medline

Hedden T, Oh H, Younger AP, Patel TA (2013) Meta-analysis of amyloid-cognition relations in cognitively normal older adults. Neurology 80:1341–1348. CrossRef Medline

Hoenig MC, Bischof GN, Hammes J, Faber J, Fliessbach K, van Eimeren T, Drzezga A (2017) Tau pathology and cognitive reserve in Alzheimer's disease. Neurobiol Aging 57:1–7. CrossRef Medline

Johnson KA, Schultz A, Betensky RA, Becker JA, Sepulcre J, Rentz D, Mormino E, Chhatwal J, Amariglio R, Papp K, Marshall G, Albers M, Mauro S, Pepin L, Alverio J, Judge K, Philiossaint M, Shoup T, Yokell D, Dickerson B, et al. (2016) Tau positron emission tomographic imaging in aging and early Alzheimer disease. Ann Neurol 79:110–119. CrossRef Medline

Josephs KA, Murray ME, Tosakulwong N, Whitwell JL, Knopman DS, Machulda MM, Weigand SD, Boeve BF, Kantarci K, Petrucelli L, Lowe VJ, Jack CR Jr, Petersen RC, Parisi JE, Dickson DW (2017) Tau aggregation influences cognition and hippocampal atrophy in the absence of beta-amyloid: a clinico-imaging-pathological study of primary age-related tauopathy (PART). Acta Neuropathol 133:705–715. CrossRef Medline

Khan UA, Liu L, Provenzano FA, Berman DE, Profaci CP, Sloan R, Mayeux R, Duff KE, Small SA (2014) Molecular drivers and cortical spread of lateral entorhinal cortex dysfunction in preclinical Alzheimer's disease. Nat Neurosci 17:304–311. CrossRef Medline

Killiany RJ, Hyman BT, Gomez-Isla T, Moss MB, Kikinis R, Jolesz F, Tanzi R, Jones K, Albert MS (2002) MRI measures of entorhinal cortex vs hippocampus in preclinical AD. Neurology 58:1188–1196. CrossRef Medline

Kivisaari SL, Probst A, Taylor KI (2013) The perirhinal, entorhinal, and parahippocampal cortices and hippocampus: an overview of functional anatomy and protocol for their segmentation in MR images. In: FMRI. Berlin, Germany: Springer Berlin Heidelberg.

Lockhart SN, Schöll M, Baker SL, Ayakta N, Swinnerton KN, Bell RK, Mellinger TJ, Shah VD, O'Neil JP, Janabi M, Jagust WJ (2017) Amyloid and tau PET demonstrate region-specific associations in normal older people. Neuroimage 150:191–199. CrossRef Medline

Logan J, Fowler JS, Volkow ND, Wang GJ, Ding YS, Alexoff DL (1996) Distribution volume ratios without blood sampling from graphical analysis of PET data. J Cereb Blood Flow Metab 16:834–840. CrossRef Medline

Maass A, Berron D, Libby L, Ranganath C, Düzel E (2015) Functional subregions of the human entorhinal cortex. ELife 4. CrossRef Medline

Maass A, Landau S, Baker SL, Horng A, Lockhart SN, La Joie R, Rabinovici GD, Jagust WJ, Alzheimer's Disease Neuroimaging Initiative (2017) Comparison of multiple tau-PET measures as biomarkers in aging and Alzheimer's Disease. Neuroimage 157:448–463. CrossRef Medline

Mitchell TW, Mufson EJ, Schneider JA, Cochran EJ, Nissanov J, Han LY, Bienias JL, Lee VM, Trojanowski JQ, Bennett DA, Arnold SE (2002) Parahippocampal tau pathology in healthy aging, mild cognitive impairment, and early Alzheimer's disease. Ann Neurol 51:182–189. CrossRef Medline

Mormino EC, Brandel MG, Madison CM, Rabinovici GD, Marks S, Baker SL, Jagust WJ (2012) Not quite PIB-positive, not quite PIB-negative: slight PIB elevations in elderly normal control subjects are biologically relevant. Neuroimage 59:1152–1160. CrossRef Medline

Olsen RK, Yeung LK, Noly-Gandon A, D'Angelo MC, Kacollja A, Smith VM,

Ryan JD, Barense MD (2017) Human anterolateral entorhinal cortex volumes are associated with cognitive decline in aging prior to clinical diagnosis. Neurobiol Aging 57:195–205. CrossRef Medline

Ossenkoppele R, Schonhaut DR, Schöll M, Lockhart SN, Ayakta N, Baker SL, O'Neil JP, Janabi M, Lazaris A, Cantwell A, Vogel J, Santos M, Miller ZA, Bettcher BM, Vossel KA, Kramer JH, Gorno-Tempini ML, Miller BL, Jagust WJ, Rabinovici GD (2016) Tau PET patterns mirror clinical and neuroanatomical variability in Alzheimer's disease. Brain 139:1551–1567. CrossRef Medline

Pernet CR, Wilcox R, Rousselet GA (2012) Robust correlation analyses: false positive and power validation using a new open source Matlab toolbox. Front Psychol 3:606. CrossRef Medline

Price JC, Klunk WE, Lopresti BJ, Lu X, Hoge JA, Ziolko SK, Holt DP, Meltzer CC, DeKosky ST, Mathis CA (2005) Kinetic modeling of amyloid binding in humans using PET imaging and Pittsburgh compound-B. J Cereb Blood Flow Metab 25:1528–1547. CrossRef Medline

Raz N, Daugherty AM, Bender AR, Dahle CL, Land S (2015) Volume of the hippocampal subfields in healthy adults: differential associations with age and a pro-inflammatory genetic variant. Brain Struct Funct 220:2663–2674. CrossRef Medline

Reitan RM, Wolfson D (1985) The Halstead-Reitan Neuropsychological Test Battery: Theory and Clinical Interpretation. Tucson, AZ: Neuropsychological Press.

Reuter M, Fischl B (2011) Avoiding asymmetry-induced bias in longitudinal image processing. Neuroimage 57:19–21. CrossRef Medline

Reuter M, Rosas HD, Fischl B (2010) Highly accurate inverse consistent registration: a robust approach. Neuroimage 53:1181–1196. CrossRef Medline

Reuter M, Schmansky NJ, Rosas HD, Fischl B (2012) Within-subject template estimation for unbiased longitudinal image analysis. Neuroimage 61:1402–1418. CrossRef Medline

Rousset OG, Ma Y, Evans AC (1998) Correction for partial volume effects in PET: principle and validation. J Nucl Med 39:904–911. Medline

Saint-Aubert L, Lemoine L, Chiotis K, Leuzy A, Rodriguez-Vieitez E, Nordberg A (2017) Tau PET imaging: present and future directions. Mol Neurodegener 12:19. CrossRef Medline

Schöll M, Lockhart SN, Schonhaut DR, O'Neil JP, Janabi M, Ossenkoppele R, Baker SL, Vogel JW, Faria J, Schwimmer HD, Rabinovici GD, Jagust WJ (2016) PET imaging of tau deposition in the aging human brain. Neuron 89:971–982. CrossRef Medline

Schwarz AJ, Yu P, Miller BB, Shcherbinin S, Dickson J, Navitsky M, Joshi AD, Devous MD Sr, Mintun MS (2016) Regional profiles of the candidate tau PET ligand 18F-AV-1451 recapitulate key features of Braak histopathological stages. Brain 139:1539–1550. CrossRef Medline

Sepulcre J, Schultz AP, Sabuncu M, Gomez-Isla T, Chhatwal J, Becker A, Sperling R, Johnson KA (2016) *In vivo* tau, amyloid, and gray matter profiles in the aging brain. J Neurosci 36:7364–7374. CrossRef Medline

Shcherbinin S, Schwarz AJ, Joshi A, Navitsky M, Flitter M, Shankle WR, Devous MD Sr, Mintun MA (2016) Kinetics of the tau PET tracer 18F-AV-1451 (T807) in subjects with normal cognitive function, mild cognitive impairment, and Alzheimer disease. J Nucl Med 57:1535–1542. CrossRef Medline

Shimada H, Kitamura S, Shinotoh H, Endo H, Niwa F, Hirano S, Kimura Y, Zhang, M.-R., Kuwabara S, Suhara T, Higuchi M (2016) Association between Aβ and tau accumulations and their influence on clinical features in aging and Alzheimer's disease spectrum brains: A [11C]PBB3-PET study. Alzheimers Dement (Amst) 6:11–20. CrossRef Medline

Small SA, Schobel SA, Buxton RB, Witter MP, Barnes CA (2011) A pathophysiological framework of hippocampal dysfunction in ageing and disease. Nat Rev Neurosci 12:585–601. CrossRef Medline

Smith A (1982) Symbol Digit Modalities Test: Manual. Los Angeles, CA: Western Psychological Services.

Sperling R, Mormino E, Johnson K (2014) The evolution of preclinical Alzheimer's disease: implications for prevention trials. Neuron 84:608–622. CrossRef Medline

Stroop JR (1938) Factors affecting speed in serial verbal reactions. Psychological Monographs 50:38–48.

Taylor KI, Probst A (2008) Anatomic localization of the transentorhinal region of the perirhinal cortex. Neurobiol Aging 29:1591–1596. CrossRef Medline

Villeneuve S, Rabinovici GD, Cohn-Sheehy BI, Madison C, Ayakta N, Ghosh PM, La Joie R, Arthur-Bentil SK, Vogel JW, Marks SM, Lehmann M, Rosen HJ, Reed B, Olichney J, Boxer AL, Miller BL, Borys E, Jin LW, Huang EJ, Grinberg LT, et al. (2015) Existing Pittsburgh compound-B positron emission tomography thresholds are too high: statistical and pathological evaluation. Brain 138:2020–2033. CrossRef Medline

Wechsler D (1997) Wechsler Memory Scale - Third Edition. San Antonio, TX: The Psychological Corporation.

Wilcox R (2004) Inferences based on a skipped correlation coefficient. J Appl Stat 31:131–143. CrossRef

Wilcox RR (2016) Comparing dependent robust correlations. Br J Math Stat Psychol 69:215–224. CrossRef Medline

Wolk DA, Das SR, Mueller SG, Weiner MW, Yushkevich PA, Yushkevich PA (2017) Medial temporal lobe subregional morphometry using high resolution MRI in Alzheimer's disease. Neurobiol Aging 49:204–213. CrossRef Medline

Wooten DW, Guehl NJ, Verwer EE, Shoup TM, Yokell DL, Zubcevik N, Vasdev N, Zafonte RD, Johnson KA, El Fakhri G, Normandin MD (2017) Pharmacokinetic evaluation of the tau PET radiotracer [18F]T807 ([18F]AV-1451) in human subjects. J Nucl Med 58:484–491. CrossRef Medline

Yushkevich PA, Pluta JB, Wang H, Xie L, Ding SL, Gertje EC, Mancuso L, Kliot D, Das SR, Wolk DA (2015) Automated volumetry and regional thickness analysis of hippocampal subfields and medial temporal cortical structures in mild cognitive impairment. Hum Brain Mapp 36:258–287. CrossRef Medline